Anion···Anion Coinage Bonds: The Case of Tetrachloridoaurate

Andrea Daolio, Andrea Pizzi, Giancarlo Terraneo, Maurizio Ursini, Antonio Frontera, and Giuseppe Resnati*

Dedicated to Professor Mir Wais Hosseini on the occasion of his 65th birthday

Abstract: *Interactions in crystalline tetrachloridoaurates of acetylcholine and dimethylpropiothetine are characterized by Au···Cl and Au···O short contacts. The former interactions assemble the $AuCl_4^-$ units into supramolecular anionic polymers, while the latter interactions append the acetylcholine and propiothetine units to the polymer. The distorted octahedral geometry of the bonding pattern around the gold center is rationalized on the basis of the anisotropic distribution of the electron density, which enables gold to behave as an electrophile (π-hole coinage-bond donor). Computational studies prove that gold atoms in negatively charged species can function as acceptors of electron density. The attractive nature of the Au···Cl/O interactions described here complement the known aurophilic bonds involved in gold-centered interactions.*

The anisotropic distribution of electron density at the outer regions of bonded atoms was first used to rationalize the noncovalent interactions formed by these atoms in the early 1990s.[1] This approach is now successfully used to explain the interactions of all groups of p-block elements in the periodic table[2] and provides valuable contributions to many fields, including catalysis,[3] drug design,[4] and crystal engineering.[5] Seven years ago, a possible extension of this mindset to d-block elements was considered[6] and subsequently confirmed, first for elements of Group 11,[7] and then for elements of Groups 10[8] and 12.[9] Various theoretical studies,[10–13] and a more limited number of experimental findings,[14,15] have

[*] A. Daolio, Dr. A. Pizzi, Prof. Dr. G. Terraneo, M. Ursini,
Prof. Dr. G. Resnati
NFMLab, Dept- Chemistry, Materials, and Chemical Engineering
"Giulio Natta"
Politecnico di Milano
via L. Mancinelli 7, 20131 Milano (Italy)
E-mail: giuseppe.resnati@polimi.it

Prof. Dr. A. Frontera
Dept. Chemistry, Universitat de les Illes Balears
Crta. de Valldemossa km 7.5
07122 Palma de Mallorca (Baleares) (Spain)

shown that nanoparticles[16] and halide salts[14] of Cu, Ag, and Au form attractive interactions with a variety of donors of electron density by involving the regions with the most positive electrostatic potential at their outer surface. It has been proposed that such interactions involving Group 11 elements should be designated as regium bonds[10] or coinage bonds.[13]

Herein we report experimental and theoretical results that show that not only gold in neutral species, as mentioned above, but also gold in negatively charged species can function as an acceptor of electron density, namely, be a coinage-bond (CiB) donor. We show that, in the solid state, $AuCl_4^-$ anions act as self-complementary tectons, with the gold and chlorine atoms functioning as CiB donor and acceptor sites, respectively. Short[17] Au···Cl contacts involving Au and Cl atoms of different units drive the formation of supramolecular anionic polymers, wherein the gold centers form a second CiB with the sp^3-hybridized oxygen atom of ester residues. Theoretical calculations prove the electrophilic role of gold as well as the attractive nature of both the Au···Cl and Au···O interactions. These findings show that CiBs involving gold(III) centers can be adaptive and robust enough to drive the formation of attractive anion···anion[18–23] and anion···neutral nucleophile[24] interactions, which determine the crystal packing of ionic derivatives.

During our studies assessing the presence of chalcogen bonds[25] and tetrel bonds[26] in bioactive molecules, we obtained the single-crystal X-ray structure of the tetrachloridoaurate salts of the methyl ester of (*S,S*)-dimethyl-β-propiothetin (**1**), an osmoregulatory and antioxidant agent in phytoplankton,[27] and of acetylcholine (**2**), a ubiquitous cholinergic neurotransmitter (Figure 1).

In the crystal packing, cationic and anionic units of **1** are connected through C−H···Cl hydrogen bonds (HBs) and a fairly linear and charge-assisted S···Cl chalcogen bond[28] (the C−S···Cl angle is 172.15°, the S···Cl separation is 358.8 pm, which corresponds to a normalized contact (Nc)[29] of 0.99; Figure S3). These interactions decrease the negative charge on the anion to the point that the gold atoms of $AuCl_4^-$ form two short contacts with two different electron-rich sites. One site is the chlorine atom of a nearby $AuCl_4^-$ anion, the other is the ester oxygen atom of a propionate unit. The Au···Cl and Au···O separations are 331.2 and 313.4 pm (the corresponding Nc values[29] are 0.85 and 0.87, respectively). The $AuCl_4^-$ anions adopt the usual square-planar conformation and the two nucleophiles get close to the gold center, almost orthogonal to the anion plane. The Cl−Au···Cl and Cl−Au···O angles span the ranges 80–100° and 85–95°,
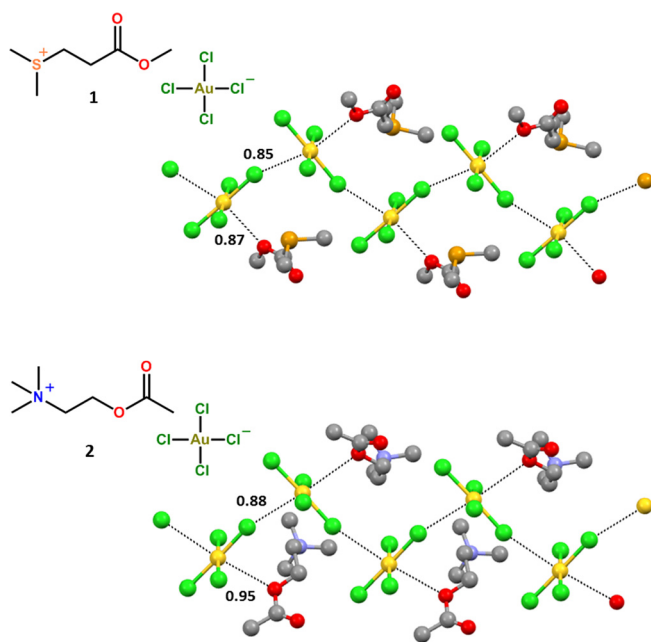
Figure 1. Structural formulas of the studied compounds and representation of anionic supramolecular polymers of **1** (top) and **2** (bottom) containing coinage bonds. CiBs are shown in black dashed lines; Nc values[29] are given; H atoms and HBs are omitted for the sake of clarity. Color code: gray, carbon; red, oxygen; light blue, nitrogen; green, chloride; yellow, gold; ocher, sulfur.[50]

thereby enabling rationalization of the Au···Cl/O interactions as π-hole[15,30] CiBs. These CiBs form an infinite supramolecular anionic chain[31–33] bearing cations as appended residues (Figure 1).

Many features of the interaction patterns in crystalline **2** are similar to those in crystalline **1**. Various C−H···Cl HBs are also present in **2** and involve hydrogen atoms geminal to the positive nitrogen atom (Figure S3). Similar to **1**, gold atoms establish a π-hole CiB with the chlorine atom of a nearby $AuCl_4^-$ anion and another π-hole CiB with the ester oxygen atom of an acetylcholine unit, thereby forming a zig-zag supramolecular anionic polymer with hanging cationic units (Figure 1). The Au···Cl and Au···O distances are 343.4 and 344.6 pm, respectively (Nc = 0.88 and 0.95, respectively); thus, they are somewhat longer than in **1**. The angular geometry of the interactions around the gold center in **2** is similar to that in **1**. Consistent with a possible nucleophilic role of the oxygen atom, the lone pair of electrons on this atom are directed towards the metal center (OC−O···Au and H_2C−O···Au angles are 109.06° and 114.77°, respectively).

Similar to what is observed even for the hard nitrogen atom in the NO_3^- anion,[34] the C−H···Cl HBs present in crystals of **1** and **2** might decrease the negative charge of the anion enough to enable the gold center in $AuCl_4^-$ to act as an electrophile. Moreover, Au is less electronegative than Cl and it can be expected that Cl−Au bonds in $AuCl_4^-$ are polarized and the net negative charge of the polyatomic anion is partitioned mostly on the chlorine atoms. The soft character of gold may favor this partitioning. Calculations were performed to support these qualitative arguments and

obtain information on Au···Cl/O interactions free from any possible crystal-packing effects.

We wondered whether the Au···Cl short contacts observed in **1** and **2** originate from packing effects (pursuing the least repulsive positioning of atoms) or whether, instead, the negatively charged $AuCl_4^-$ molecular entities can act as π-holes (that is, can attractively interact with Lewis bases). Consequently, the theoretical study was initially focused on analysing the molecular electrostatic potential (MEP) surfaces of the $AuCl_4^-$ unit and the entire salts. The MEP results are summarized in Table 1 and Figure 2, where only the results for **2** are shown. The MEP surface of **1** is shown in the Supporting Information (Figure S4).

As expected, the MEP values of the isolated anion are negative over the entire surface because of its net negative charge, and the global minimum is found along the bisector of the Cl-Au-Cl angle. There are two regions where the MEP values are at a maximum (less negative), which are at the extensions of the four Au−Cl bonds (σ-holes)[30] and above

Table 1: MEP values (in kcal mol⁻¹) of the $AuCl_4^-$ anion and compounds **1** and **2** at the σ-holes of Cl and π-holes of Au atoms using different isovalues (a.u.) for the electron density.

Cmpd[a]	Isovalue (% e in the surface)			
	0.001 (99.0)	0.002 (98.2)	0.004 (96.7)	0.008 (94.2)
$AuCl_4^-$; σ(Cl)	−79.6	−79.6	−77.8	−70.2
$AuCl_4^-$; π(Au)	−78.3	−74.6	−67.8	−54.8
1; σ(Cl)	−30.5	−29.7	−26.3	−15.7
1; π(Au)	−25.1	−20.5	−12.6	+2.0
2; σ(Cl)	−27.0	−24.8	−19.4	−10.0
2; π(Au)	−20.1	−14.4	−6.0	+9.1

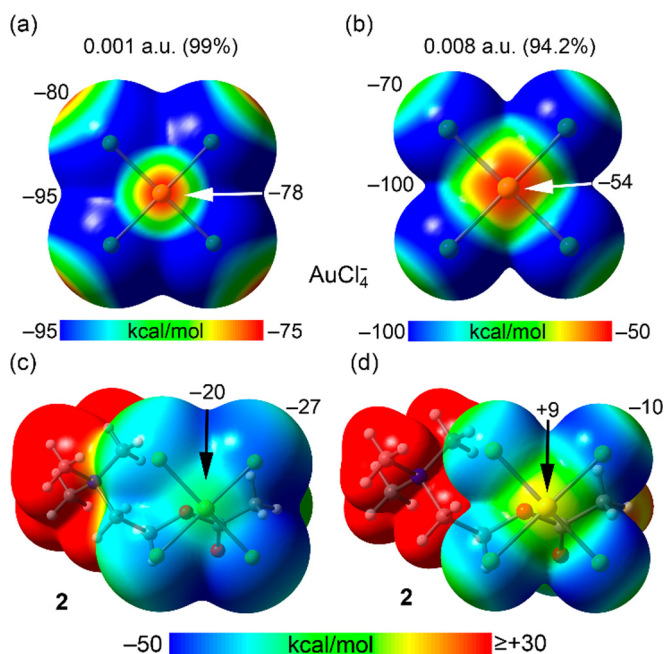[a] π and σ stand for π-hole and σ-hole, respectively.

Figure 2. MEP surfaces of the $AuCl_4^-$ unit and **2** using 0.001 a.u. (a and c) and 0.008 a.u. (b and d) isovalues at the PBE0-D3/def2-TZVP level of theory. The values are given in kcal mol⁻¹ at some points of the surface.

and below the Au atom (π-holes, the terms σ/π-hole are used also for regions with negative potential[20,23,30]). The MEP values are similar at both types of holes (−79.6 and −78.3 kcal mol⁻¹ for σ and π-holes, respectively). The MEP surface analysis of the salt (**2**) shows that the value of the potential at the π-hole of the Au center, while remaining negative, is reduced to −20.1 kcal mol⁻¹. At this point, it is interesting to comment on the influence of the isovalue used to construct the MEP surface on the energy values at the σ,π-holes. Based on Bader's recommendation,[35] the surface generated using the 0.001 a.u. isovalue (embraces 99% of the electron density) is the best estimate of the van der Waals surface. Examination of the interactions discussed above reveals that the Au⋯O/Cl distances are shorter than the sum of the corresponding van der Waals radii (Nc < 1). Therefore, to better rationalize the solid-state behavior of these compounds it might be beneficial to investigate the effect of increased isovalues (i.e. reduce the volume of the surface). The results are given in Table 1 and Figure 2, and it can be observed that the MEP values at both the σ and π-holes progressively become more positive as the isovalue increases (volume decreases). The effect on the π-hole is more significant than that on the σ-hole. Interestingly, for the 0.008 a.u. isovalue, where the size of the surface is reduced by approximately 5%, the MEP value at the π-hole becomes positive, whilst that at the σ-hole remains negative. Since the experimental Au⋯Cl distances in **1** and **2** are up to 15% shorter than the sum of the van der Waals radii, it is reasonable to anticipate the electrophilic role of the Au centers in the Au⋯Cl contacts observed in the solid state of both compounds. Further analysis of the importance of electrostatic effects is given in the Supporting Information (Section S4.2, Figures S5 and S6), where the results from the energy decomposition analyses of the anion⋯anion and cation⋯anion dimers are described.

For both complexes, the Au⋯O/Cl contacts were further characterized by using the quantum theory of "atoms-in-molecules" (QTAIM) and the noncovalent interaction index (NCIplot). Analyses of ternary assemblies retrieved from the X-ray structures are given in Figure 3, including their formation energies. The QTAIM analysis confirms the existence of the Au⋯O/Cl contacts, each one characterized by a bond critical point (CP) and a bond path connecting the Au atom to the Cl or O atom. The analysis also reveals the existence of several C−H⋯Cl contacts showing bond CPs and bond paths connecting the C−H bonds to the Cl atoms (see Figure 3). The presence of Au⋯O/Cl and C−H⋯Cl interactions is also confirmed by the NCIplot analysis, which reveals the existence of green or bluish isosurfaces (meaning attractive interactions) located between the interacting atoms. The electron density values (ρ) at the bond CPs (indicated in italics in Figure 3) suggest that the π-hole interactions are stronger in **1**, in line with their shorter distances (smaller Nc values, Figure 1). In contrast, the formation energy for the trimeric assembly of **2** (ΔE_2 = −61.3 kcal mol⁻¹) is larger than that of **1** (ΔE_1 = −50.9 kcal mol⁻¹), likely due to the contribution of the HBs, which are more numerous in **2**. The interaction energies of the two dimers that constitute the trimers are also indicated in
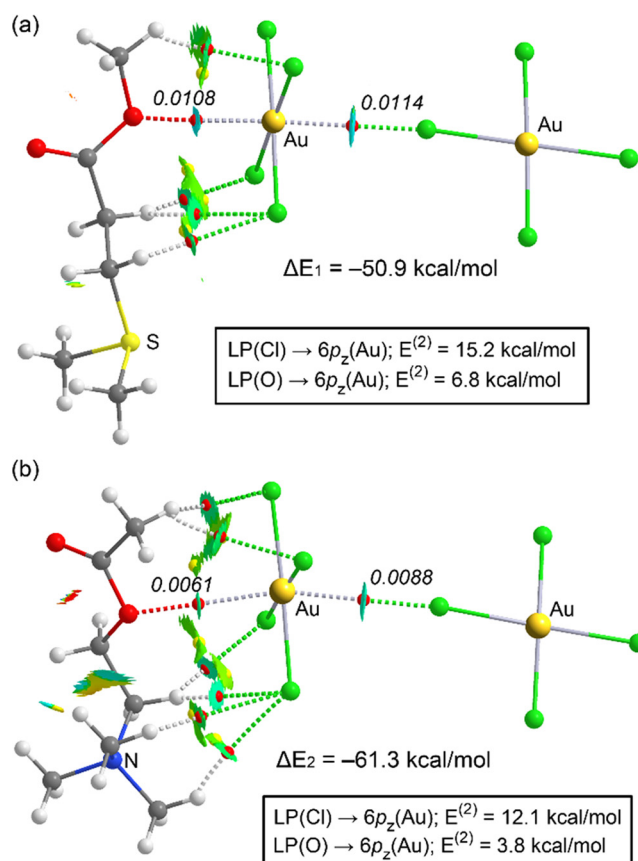

Figure 3. QTAIM distribution of the critical points of the intermolecular bond and ring (red and yellow spheres, respectively) and bond paths for the trimeric assemblies of compounds **1** (a) and **2** (b). The density at the bond CPs that characterize the CiBs are given in italics (a.u.) The superimposed NCIplot isosurface (RDG isovalue = 0.4 a.u.) is shown. The cut-off ρ = 0.04 a.u. has been used. Color range: −0.02 a.u. ≤ (signλ2)ρ ≤ 0.02. Level of theory: PBE0-D3/def2-TZVP. The second-order perturbation energies E$^{(2)}$ along with the donor and acceptor orbitals obtained from the NBO analysis are indicated.

Figure 3, and show that the ion-pair interaction is stronger in **2** (more C−H⋯Cl contacts), whilst the repulsive anion⋯anion interactions are very similar (ca. +47 kcal mol⁻¹). This positive value is significantly smaller than the electrostatic repulsion of two point charges of the same sign located at the center of masses of both molecules (60.0 and 58.6 kcal mol⁻¹ for **1** and **2**, respectively).

We have also studied if orbital contributions are important in the π-hole Au⋯O/Cl interactions described above. For this purpose, a natural bond orbital (NBO) second-order perturbation analysis has been carried out, since it is convenient for analysing donor–acceptor interactions.[36] Remarkably, the calculations reveal significant orbital contributions in both complexes (Figure 3). These contributions come from electron donations from one lone pair (LP) of electrons on the chlorine or oxygen atoms to the empty $6p_z$ atomic orbital of Au. The second-order stabilization energies E$^{(2)}$ associated with the orbital donor–acceptor interactions are also indicated in Figure 3. The LP(Cl)→$6p_z$(Au) donation is stronger than the LP(O)→$6p_z$(Au) donation in both complexes, consistent with the Nc values of the corresponding

interactions in the crystals (the plots of the donor–acceptor NBOs are given in Figure S7). Moreover, the NBO analysis confirms that both CiBs are stronger in **1** than in **2**, in agreement with the QTAIM results and geometric features of the interactions. Finally, the NBO analysis confirms the π-hole nature of the interaction, where the Au atom acts as an acceptor and the Cl/O atoms act as donors of electron density.

A similar analysis was then performed for the ChB observed in crystalline propiothetin derivative **1** (Figure S8). The NBO analysis confirms a minor LP(Cl)→σ*(S-C) orbital contribution, representative of a weak ChB. The second-order stabilization energies $E^{(2)}$ associated with this interaction are 0.7 kcal mol^{-1}, in line with the long distance between the two atoms.

The Au···nucleophile contacts observed in **1** and **2** are the shortest in the reported crystals. In **1**, the second shortest interaction is a C−H···O HB having an Nc of 0.88 (the mean Nc of all HBs is 0.93). A similar situation is shown in **2** (the Nc of the shortest HB is 0.92, whereas the mean Nc of all HBs is 0.95). Clearly, the CiBs formed by $AuCl_4^-$ anions are structural determinants of the crystal packing of **1** and **2**, and the Cambridge Structural Database (CSD) suggests that this behavior may be quite general in crystals. A CSD analysis reveals that short and orthogonal Au···nucleophile contacts are present in nearly one third of the structures containing the $AuCl_4^-$ anion (Tables S13 and S14). In most cases, the nucleophile is a chlorine atom of an adjacent $AuCl_4^-$ unit,[31–33] but it can also be a Cl^- anion[37] or a neutral atom that possesses a lone pair of electrons (e.g. the oxygen atom of an *S*-oxide,[38] *N*-oxide,[39] nitro,[40] or ether[41] group). Similar short and orthogonal Au···nucleophile contacts are formed in the solid state by anions of other Au^{III} salts, for example, $AuBr_4^-$[42] and $Au(CN)_4^-$[43] (Tables S15 and S16).

In conclusion, experimental evidence is given that the gold atom of $AuCl_4^-$ anions form short contacts with both neutral and anionic nucleophiles in the solid state. Computations show that these interactions are attractive, and their orthogonal directionality is consistent with π-hole CiBs.[15] Anion···anion interactions enabled by hydrogen bonds,[44] halogen bonds,[45] or involving perhalometallate anions of Groups 2,[46] 3,[24] and 12[20,23] elements have been rationalized by anisotropic distribution of the electron density in the anions. Interestingly, the same theoretical approach was used to analyze the effects overcoming anion–anion Coulomb repulsions and allowing the formation of stable adducts $PnCl_4^-$···CN^- (Pn = P, As, Sb), wherein the $PnCl_4^-$ anion adopts a square-planar geometry similar to that of $AuCl_4^-$.[47] The experimental and theoretical results reported here prove that anion···anion interactions involving $AuCl_4^-$ are reliable and robust supramolecular synthons that consistently control the interactions in crystalline structures. The use of these interactions in the design and control of structural features of materials may allow a fine-tuning of their functional properties, for example, in perovskites for solar cells[42] or ambient pressure superconductors[39] that contain $AuCl_4^-$ anions. Analogous interactions occurring in solution may account for the Lewis acid catalytic activity of the tetrachloroaurate anion.[48] The π-hole CiBs reported here (involving gold(III) derivatives) are a valuable extension of the applicative

potential of gold interactions, which are currently dominated by aurophilic bonds (involving gold(I) derivatives).[49]

Conflict of interest

The authors declare no conflict of interest.

[1] T. Brinck, L. S. Murray, P. Politzer, *Int. J. Quantum Chem.* **1992**, *44*, 57–64.

[2] P. Scilabra, G. Terraneo, G. Resnati, *Acc. Chem. Res.* **2019**, *52*, 1313–1324.

[3] S. Benz, A. I. Poblador-Bahamonde, N. Low-Ders, S. Matile, *Angew. Chem. Int. Ed.* **2018**, *57*, 5408–5412; *Angew. Chem.* **2018**, *130*, 5506–5510.

[4] V. R. Mundlapati, D. K. Sahoo, S. Bhaumik, S. Jena, A. Chandrakar, H. S. Biswal, *Angew. Chem. Int. Ed.* **2018**, *57*, 16496–16500; *Angew. Chem.* **2018**, *130*, 16734–16738.

[5] V. Kumar, D. L. Bryce, *Cryst. Growth Des.* **2020**, *20*, 2027–2034.

[6] G. Cavallo, P. Metrangolo, T. Pilati, G. Resnati, G. Terraneo, *Cryst. Growth Des.* **2014**, *14*, 2697–2702.

[7] J. H. Stenlid, T. Brinck, *J. Am. Chem. Soc.* **2017**, *139*, 11012–11015.

[8] G. Li, J. H. Stenlid, M. S. G. Ahlquist, T. Brinck, *J. Phys. Chem. C* **2020**, *124*, 14696–14705.

[9] A. Bauzá, I. Alkorta, J. Elguero, A. Frontera, *Angew. Chem. Int. Ed.* **2020**, *59*, 17482–17487; *Angew. Chem.* **2020**, *132*, 17635–17640.

[10] R. Wang, Z. Wang, X. Yu, Q. Li, *ChemPhysChem* **2020**, *21*, 2426–2431.

[11] W. Zierkiewicz, M. Michalczyka, S. Scheiner, *Phys. Chem. Chem. Phys.* **2018**, *20*, 22498–22509.

[12] C. Trujillo, G. Sánchez-Sanz, J. Elguero, I. Alkorta, *Struct. Chem.* **2020**, *31*, 1909–1918.

[13] A. Frontera, A. Bauzà, *Chem. Eur. J.* **2018**, *24*, 7228–7234.

[14] A. C. Legon, N. R. Walker, *Phys. Chem. Chem. Phys.* **2018**, *20*, 19332–19338.

[15] A. Terrón, J. Builsa, T. J. Mooibroek, M. Barceló, O. A. Garcí-Raso, J. J. Fiol, A. Frontera, *Chem. Commun.* **2020**, *56*, 3524–3527.

[16] J. Halldin Stenlid, A. J. Johansson, T. Brinck, *Phys. Chem. Chem. Phys.* **2018**, *20*, 2676–2692.

[17] The wording short, or close, contacts is used for interactions wherein the separation of the involved atoms is shorter than the sum of the van der Waals radii (or anionic Pauling radii if anions are involved).

[18] Y. V. Nelyubina, M. Y. Antipin, K. A. Lyssenko, *Russ. Chem. Rev.* **2010**, *79*, 167–187.

[19] S. R. Kass, *J. Am. Chem. Soc.* **2005**, *127*, 13098–13099.

[20] R. Wysokiński, W. Zierkiewicz, M. Michalczyk, S. Scheiner, *ChemPhysChem* **2021**, *22*, 818–821.

[21] T. Maxson, A. S. Jalilov, M. Zeller, S. V. Rosokha, *Angew. Chem. Int. Ed.* **2020**, *59*, 17197–17201; *Angew. Chem.* **2020**, *132*, 17350–17354.

[22] D. A. Cullen, M. G. Gardiner, N. G. White, *Chem. Commun.* **2019**, *55*, 12020–12023.

[23] R. Wysokiński, W. Zierkiewicz, M. Michalczyk, S. Scheiner, *ChemPhysChem* **2020**, *21*, 1119–1125.

[24] R. Wysokiński, M. Michalczyk, W. Zierkiewicz, S. Scheiner, *Phys. Chem. Chem. Phys.* **2021**, *23*, 4818–4828.

[25] A. Daolio, P. Scilabra, M. E. Di Pietro, C. Resnati, K. Rissanen, G. Resnati, *New J. Chem.* **2020**, *44*, 20697–20705.

[26] V. Kumar, P. Scilabra, P. Politzer, G. Terraneo, A. Daolio, F. Fernandez-Palacio, J. S. Murray, G. Resnati, *Cryst. Growth Des.* **2021**, *21*, 642–652.

[27] M. Vila-Costa, R. Simó, H. Harada, J. M. Gasol, D. Slezak, R. P. Kiene, *Science* **2006**, *314*, 652–654.

[28] C. Aakeroy, D. L. Bryce, G. R. Desiraju, A. Frontera, A. C. Legon, F. Nicotra, K. Rissanen, S. Scheiner, G. Terraneo, P. Metrangolo, G. Resnati, *Pure Appl. Chem.* **2019**, *91*, 1889–1892.

[29] The "normalized contact" Nc for an interaction involving atoms i and j is the ratio $D_{ij}/(rvdW,i + rvdW,j)$, where D_{ij} is the experimental distance between i and j and rvdW,i and rvdW,j are the van der Waals radii of i and j. If the electron donor j is an anionic atom, rvdW,j is substituted by the Pauling ionic radius of the anion atom j. The radii 210, 181, and 152 pm are used here for Au, Cl⁻, and O, respectively.

[30] J. S. Murray, P. Lane, T. Clark, K. E. Riley, P. Politzer, *J. Mol. Model.* **2012**, *18*, 541–548.

[31] M. Hasan, I. V. Kozhevnikov, M. R. H. Siddiqui, A. Steiner, N. Winterton, *Inorg. Chem.* **1999**, *38*, 5637–5641.

[32] L. E. Pope, J. C. A. Boeyens, *J. Cryst. Mol. Struct.* **1975**, *5*, 47.

[33] D. Paliwoda, M. Szafranski, M. Hanfland, A. Katrusiak, *J. Mater. Chem. C* **2018**, *6*, 7689–7699.

[34] A. Bauza, A. Frontera, T. J. Mooibroek, *Nat. Commun.* **2017**, *8*, 14522.

[35] R. F. W. Bader, *Chem. Rev.* **1991**, *91*, 893–928.

[36] E. D. Glendening, C. R. Landis, F. Weinhold, *Wiley Interdiscip. Rev.: Comput. Mol. Sci.* **2012**, *2*, 1–42.

[37] E. V. Makotchenko, I. A. Baidina, L. A. Sheludyakova, *Zh. Strukt. Khim.* **2012**, *53*, 1164–1170.

[38] Yu. A. Simonov, L. I. Budarin, A. A. Dvorkin, T. I. Malinovskii, E. V. Fesenko, S. V. Pavlova, *Kristallografiya* **1987**, *32*, 905–910.

[39] T. Asaji, E. Akiyama, F. Tajima, K. Eda, M. Hashimoto, Y. Furukawa, *Polyhedron* **2004**, *23*, 1605–2213.

[40] M. Calleja, K. Johnson, W. J. Belcher, J. W. Steed, *Inorg. Chem.* **2001**, *40*, 4978–4985.

[41] T. K. Hagos, S. D. Nogai, L. Dobrzanska, S. Cronje, H. G. Raubenheimer, *Acta Crystallogr. Sect. E* **2009**, *65*, m255–m256.

[42] C. Worley, A. Yangui, R. Roccanova, M.-H. Du, B. Saparov, *Chem. Eur. J.* **2019**, *25*, 9875–9884.

[43] T. Shirahata, M. Kibune, H. Yoshino, T. Imakubo, *Chem. Eur. J.* **2007**, *13*, 7619–7630.

[44] I. Mata, E. Molins, I. Alkorta, E. Espinosa, *J. Phys. Chem. A* **2015**, *119*, 183–194.

[45] Y. Li, L. Meng, Y. Zeng, *ChemPhysChem* **2021**, *22*, 232–240.

[46] W. Zierkiewicz, R. Wysokinski, M. Michalczyk, S. Scheiner, *ChemPhysChem* **2020**, *21*, 870–877.

[47] S. Scheiner, R. Wysokinski, M. Michalczyk, W. Zierkiewicz, *J. Phys. Chem. A* **2020**, *124*, 4998–5006.

[48] A. S. K. Hashmi, *Chem. Rev.* **2007**, *107*, 3180–3211.

[49] H. Schmidbaur, A. Schiera, *Chem. Soc. Rev.* **2012**, *41*, 370–412.

[50] CCDC 2075035 (**1**) and 2075038 (**2**) contains the supplementary crystallographic data for this paper. These data can be obtained free of charge via www.ccdc.cam.ac.uk/conts/retrieving.html (or from the Cambridge Crystallographic Data Centre, 12, Union Road, Cambridge CB21EZ, UK; fax: (+44)1223-336-033; or deposit@ccdc.cam.ac.uk).